AN INNOVATIVE ROUTE FROM WIND TUNNEL EXPERIMENTS TO FLIGHT DYNAMICS ANALYSIS FOR A HIGHLY SWEPT FLYING WING

J. Schwithal, D. Rohlf
DLR Institute of Flight Systems,
Lilienthalplatz 7, 38108 Braunschweig, Germany

G. Looye
DLR Institute of System Dynamics and Control,
Münchener Straße 20, 82234 Weßling, Germany

C. M. Liersch
DLR Institute of Aerodynamics and Flow Technology,
Lilienthalplatz 7, 38108 Braunschweig, Germany

Abstract

A flying wing configuration with highly swept leading edges and low aspect ratio such as the generic UCAV configuration DLR-F19 is very attractive for military applications due to its very favorable stealth capabilities. As the assurance of good flying qualities, however, is a critical aspect for such a configuration, it should be considered early in the design process. This paper presents an innovative way to derive a flight dynamics model from wind tunnel experiments by applying a system identification approach, normally employed for flight test. This allows the modelling of nonlinear aerodynamic effects and provides a model which can be directly integrated into flight dynamics simulations. New wind tunnel maneuvers are applied which significantly reduce the time of the wind tunnel experiments and improve the quality of the aerodynamic dataset generation. The aerodynamic model is then integrated into a 6-DoF simulation environment in order to perform a flight dynamics analysis of the UCAV configuration. The purpose of this analysis is to compare the flying qualities as derived from wind tunnel data with the results determined on the basis of data from VSAERO, a low-fidelity aerodynamic tool used in preliminary aircraft design.

LIST OF SYMBOLS

α	angle of attack, [°]
β	angle of sideslip, [°]
Φ	bank angle, [°]
Φ_t	critical bank angle for roll performance, [°]
ω_0	natural frequency, [rad/s]
C_i	coefficient of force or moment i, [-]
C_{i0}	basic coefficient of force or moment i, [-]
C_{ij}	nondimensional derivative of force or moment i with respect to j, [-]
D	damping ratio, [-]
F_{vD}	vortex drag factor, [-]
f_0	model oscillation frequency, [Hz]
f_s	sampling frequency, [Hz]
g	gravity constant, [m/s²]
I_{xx}, I_{yy}, I_{zz}	moment of inertia in x/y/z-axis, [kg m²]
L, D, Y	aerodynamic lift, drag and side force [N]
L_β, N_β	dimensional roll and yaw moment derivative with respect to sideslip angle, [1/s²]
l, m, n	aerodynamic moments, [Nm]
N_r	dimensional yaw moment derivative with respect to roll rate, [1/s]
n_z	vertical load factor, [-]
p, q, r	roll rate, pitch rate, yaw rate, [rad/s]
T_2	time to double amplitude, [s]
t	time, [s]
Y_β, Y_{rud}	dimensional side force derivative with respect to sideslip angle and rudder deflection, [1/s]

LIST OF ABBREVIATIONS

AC	AirCraft
AVT	Applied Vehicle Technology
CAP	Control Anticipation Parameter
CFD	Computational Fluid Dynamics
CPACS	Common Parametric Aircraft Configuration Schema
DAMIP	Dynamic Aircraft Model Integration Process
DNW	German–Dutch Wind Tunnels
DoF	Degrees of Freedom
HAREM	HAndling qualities Reasearch using Matlab
LIB	Left InBoard control surface
LOB	Left OutBoard control surface
LSP	Left SPlit flaps
MPM	Model Positioning Mechanism
NASA	National Aeronautics and Space Administration
NATO	North Atlantic Treaty Organization
NWB	Low-Speed Wind Tunnel Braunschweig
RANS	Reynolds-averaged Navier-Stokes
RIB	Right InBoard control surface
ROB	Right OutBoard control surface
RSP	Right SPlit flaps
RTO	Research and Technology Organisation
SACCON	Stability And Control CONfiguration
STO	Science and Technology Organization
SysID	System IDentification
UCAV	Unmanned Combat Aerial Vehicle

LIST OF INDICES

a	aerodynamic coordinate system
ail	aileron
b	body-fixed coordinate system
dr	Dutch roll
hys	hysteresis
rud	rudder
SP	short period

1. INTRODUCTION

The DLR-F19 configuration (Figure 1) is a highly swept flying wing with a low aspect ratio and a partially round and partially sharp leading edge. It has the same lambda-wing planform as the SACCON (Stability And Control CONfiguration) wind tunnel model built by NASA, but different control surfaces. The configuration was established within the NATO/RTO Task group AVT-161 "Assessment of Stability and Control Prediction Methods for NATO Air and Sea Vehicles" [1] and has extensively been analyzed concerning different disciplines at DLR.

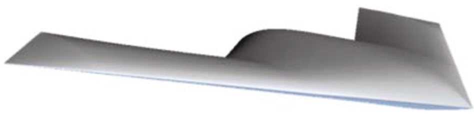

FIGURE 1. DLR-F19 configuration

A detailed description of the configuration and its design process can be found in [2]. A large benefit of the configuration is its favorable stealth capability resulting from its planform with parallel edges, which makes it an attractive candidate as a future UCAV (Unmanned Combat Aerial Vehicle) for military applications. Concerning the aerodynamic analysis and the assurance of an adequate flight dynamic behavior perspective, however, the configuration is quite challenging. The flow field around the configuration is dominated by vortex structures and vortex-to-vortex interactions. The aerodynamic behavior is thus strongly nonlinear and difficult to predict with analytical approaches. Wind tunnel experiments have been conducted to study these complex aerodynamics and to provide a solid aerodynamic database.

In order to use these data of the wind tunnel experiments for flight dynamics simulations, they have to be converted into an aerodynamic model first. In the case of nonlinear aerodynamics this is nontrivial. The approach presented in this paper is based on a system identification method, as it is usually employed for flight test, to determine the static and dynamic derivatives of the configuration and to develop an aerodynamic model.

Static or stability derivatives are the rates of change of aerodynamic force and moment coefficients with respect to linear or angular velocity components. Dynamic derivatives are the time derivatives thereof. They are needed for the determination of stability and control characteristics of an aircraft; they are also required for load assessment of individual airplane components and finally for the validation of numerical codes.

Dynamic derivatives are usually tested in wind tunnels incorporating special wind tunnel models as well as dedicated test rigs enabling sinusoidal oscillations of the wind tunnel model. A classic method is to employ linear aerodynamic models. However, this approach is not ideally suited for an extended flight envelope. Furthermore, it is rather time consuming. Therefore sinusoidal oscillations have been replaced with suitable maneuvers in the wind tunnel here and system identification has been applied to calculate dynamic derivatives.

An alternative approach to model the aerodynamic behavior of an aircraft is the numerical calculation of the aerodynamic coefficients. When using RANS (Reynolds-averaged Navier-Stokes)-based high-fidelity CFD methods, these computations can be very expensive in terms of time and computational costs. An alternative, typically used in the early phases of aircraft design, is to use methods which are based on simplified flow equations. One of these methods is VSAERO [3], a classical 3D panel method based on the linearized potential flow equation. Using such a fast and robust method, it is possible to create a comprehensive database for flight dynamics investigations automatically and within only a few hours of time. Certainly the aerodynamic dataset generated with VSAERO is not able to cover all effects of the complex aerodynamics of the considered UCAV configuration. Nevertheless, it shall be applied here in order to investigate whether this approach is suitable to get first insights of the flight dynamic behavior of the aircraft – at least for low angles of attack. If so, this would be very beneficial for the early stages of design, when the geometry still changes permanently.

A comparison between the aerodynamic data determined with VSAERO and the aerodynamic dataset derived from the wind tunnel experiments is accomplished by applying different flying qualities criteria to flight dynamics models created from the two different datasets.

For the numerical analysis of the UCAV configuration the aircraft is modelled in the CPACS (Common Parametric Aircraft Configuration Schema) data format [4]. CPACS is a data definition developed at DLR for the description of aircraft related data. It serves as a common language and an interface which allows exchanging information between different tools within the aircraft design process. The VSAERO computations as well as the generation of the flight dynamics model and the flying qualities analysis presented in sections 3, 4 and 5 are all performed on the basis of the common CPACS file containing the UCAV configuration.

2. WIND TUNNEL EXPERIMENTS

2.1. Test Facility

The tests described herein have been performed in the Low-Speed Wind Tunnel Braunschweig (NWB), belonging to the German-Dutch Wind Tunnels (DNW). The DNW-NWB is an atmospheric low-speed wind tunnel, which has recently been refurbished to become an aero-acoustic facility. Detailed information about the DNW-NWB can be found in [5], [6] and [7].

The model is mounted by means of a ventral sting on NWB's Model Positioning Mechanism MPM (Figure 2). The MPM can be described as a 6-degrees-of-freedom (DoF) parallel kinematics system incorporating six struts of constant length whose joints at the wind tunnel fixed side connect to six electric linear motors and on the other side connect to the *Stewart platform*, thereby obtaining three translatory and three rotatory degrees of freedom. The electric linear motors traverse along two rails, which are, like the Stewart platform, located above the test section. The MPM can be employed in combination with the open or closed test section configuration. The MPM can be used for high precision static model positioning as well as for arbitrary pre-defined maneuvers within its working space including sinusoidal model oscillations.

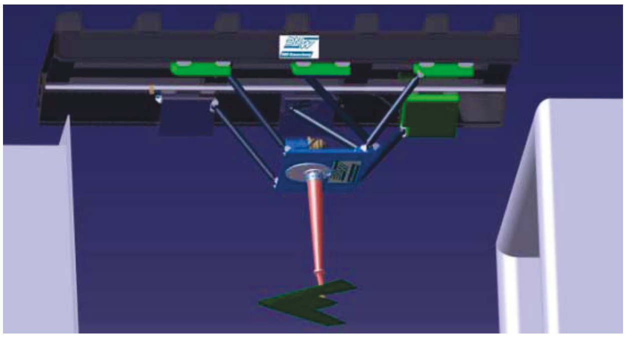

FIGURE 2. Sketch of the Model Positioning Mechanism (MPM) in the DNW-NWB wind tunnels

In order to augment the working space about model-fixed pitch and roll axes an additional electric actuator is mounted on the Stewart platform, controlled by the same software as the linear motors ("7th axis"). The frequency can be set continuously from f_0 = 0.0 Hz to f_0 = 3.0 Hz. In general, the amplitude range depends on the frequency, the oscillation type and on the balance mount. The development of the dynamic testing systems at DNW-NWB, leading finally to the MPM, is described in [8].

2.1.1. Wind Tunnel Model

The DLR-F19 wind tunnel model, together with its predecessor, the NASA built SACCON of identical planform and only slightly different control surfaces, is a generic UCAV configuration with a 53° leading edge sweep and a lambda wing planform, as shown in Figure 3. The model has been made from carbon fiber composite material in order to keep the model weight as low as possible, consequently reducing inertial forces and moments. The combination of high stiffness and low weight also leads to eigenmode frequencies which are in the order of one magnitude above the intended oscillation frequencies.

The design and manufacture of the DLR-F19 model as well as the wind tunnel tests at DNW-NWB have been performed within the NATO STO AVT-201 Task Group "Extended Assessment of Stability and Control Prediction Methods for NATO Air Vehicles" [9], [10].

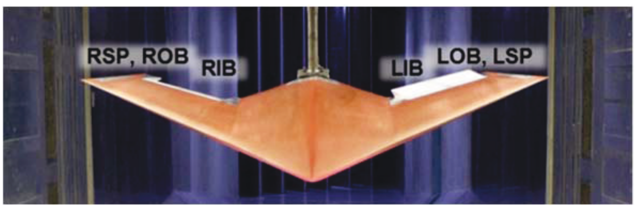

FIGURE 3. DLR-F19 in the DNW-NWB closed test section (mounted top down on a belly sting). LIB/LOB label the left inboard/outboard flaps and RIB/ROB the right inboard/outboard flaps, respectively. RSP/LSP stands for right and left split flaps.

2.1.2. Maneuver Generation

During flight tests, the aircraft motion is induced by control surface deflections which are defined in order to permit an adequate identifiability. In the wind tunnel, the excitation of the model motion is performed directly by the MPM applying fixed control surface deflections. Apart from sinusoidal oscillations at fixed reference conditions, the MPM can execute arbitrary maneuvers, which are optimized for parameter identification purposes in this case. The time step does not have to be constant but can be – even within one maneuver definition – adapted to the accelerations which have to be resolved. The smallest possible time step is 10 ms. The maximum number of time steps depends on the maneuver definition.

For the latest test campaign with the DLR-F19 model, new quasi-steady maneuvers with superimposed harmonic excitations or frequency sweeps were designed to significantly reduce the time for the wind tunnel experiments and to improve the quality of the aerodynamic dataset generation based on nonlinear parameter identification methods. All maneuvers performed are based on a "1 – cosine" α-sweep generated by the Stewart platform and the 7th axis of the MPM leading to a total angle of attack range of roughly α = -5° to α = 25°. Harmonic oscillations of either constant or varying frequency can be superimposed to this quasi-steady α-sweep. Furthermore, the MPM permits to superimpose motions about other axes, e.g. rolling or yawing oscillations. This has been realized during other test campaigns.

2.1.3. Data Acquisition

Data acquisition for all dynamic tests was performed using a data acquisition system with a sampling frequency of f_s = 600 Hz. No corrections for wall or blockage effects were applied to the forced motion time history data. The model's attitude was measured with a pair of video cameras, evaluating the location of markers applied to the model surface at the same sampling frequency. The calculation of the derivatives is based on the assumption that the wind tunnel model is ideally stiff. All tests are performed around symmetrical flow conditions (β_0 = 0).

For the further data evaluation the mass and inertial forces and moments, always contained in the recorded signals in wind-on conditions when the model performs an unsteady motion, have to be eliminated. This can be achieved by performing measurements with the model executing exactly the same oscillation (or maneuver) in wind-off conditions. In case of the Fourier analysis, the wind-off data is subtracted from the wind-on data after the Fourier coefficients (described in [11]) have been calculated. In case of evaluation by parameter estimation, this subtraction is performed prior to the estimation.

2.2. Data Evaluation

2.2.1. Classical Approach

The classical approach assumes that the aerodynamic forces and moments are linear functions of model attitude and angular speed, or, at heave and lateral oscillation, linear functions of translatory speed and acceleration. Several methods for the calculation of dynamic derivatives based on a linear assumption exist [12].

For a pitching oscillation, the Fourier analysis according to

[11] yields the following pitching moment derivatives: C_{m_0}, C_{m_α} and $C_{m_{\dot\alpha}} + C_{m_q}$ as well as the corresponding derivatives for C_X and C_Z. The result of a linear analysis, taking only the fundamental frequency into account, is given in [13]. It clearly indicates the inadequate representation of nonlinear aerodynamic data.

2.2.2. System Identification

2.2.2.1. General Approach

Early in 2009, DLR investigated the general applicability of its system identification (SysID) method to dynamic wind tunnel data, demonstrating that the application of linear aerodynamic models is principally possible but has only limited potential. The core of the Matlab/Simulink®-based SysID procedure [14] is an output error parameter estimation algorithm, which was used in this application to minimize the differences between model-fixed measured and simulated forces and moments or their respective coefficients. While the parameters appearing in the aerodynamic model are estimated with a standardized procedure, the model structure itself must be developed through engineering judgment and reasoning.

In the present system identification application, DLR developed an equivalent nonlinear aerodynamic model to enable real-time 6-DoF flight mechanical simulations. This implies that the stability parameters can be predicted at intermediate angle-of-attack values (and oscillation frequencies). The essential advantage of the 6-DoF approach is the fact that a single set of aerodynamic coefficients/derivatives covers the entire tested angle of attack regime, accounting additionally for aerodynamic cross couplings.

2.2.2.2. Nonlinear Approach

Whilst the linear approach may give good reliable results for the low α regime where the flow is relatively steady, it is likely to be unsuitable for modeling the more complex effects of the turbulent or detached flow at higher α. The nonlinear approach in this paper addresses this by using a more general nonlinear model. This model was developed to provide the approximation of the aerodynamic total aircraft coefficients without direct modeling of the vortical airflow characteristics (so called equivalent modeling).

The six equations are based on a number of angle-of-attack breakpoints to cope with the nonlinearities in the angle-of-attack dependencies. In between these breakpoints the corresponding derivative is linearly interpolated. The breakpoints themselves are estimated along with the aerodynamic parameters so as to be automatically concentrated in the areas with significant changes of the angle-of-attack-dependent derivatives. A simple smoothing function is applied to the total coefficients in order to remove excessive peaks, i.e. each data value is adjusted depending on the spacing of the associated angle-of-attack value to the preceding and succeeding angle-of-attack breakpoints. The derivatives are linear with respect to the other input signals, which are β, p, q, r, and angle of attack rate $\dot\alpha$ The rates are calculated in a pre-processing step by means of numerical differentiation. In the case of plunge tests, the difference $\dot\alpha$-q is used to avoid high correlations during the estimation of $\dot\alpha$ and q derivatives. In all other test cases, the signals of $\dot\alpha$ and q are identical.

Drag is modeled as a function of lift to the power of 4 scaled by a 'vortex drag factor' F_{vD}, which is to be estimated. In the longitudinal equations, the high lift hysteresis formula suggested in [15] and [16] is used in addition, influencing primarily lift, but also drag and pitching moment. A detailed description of the equivalent aerodynamic model equations can be found in [13].

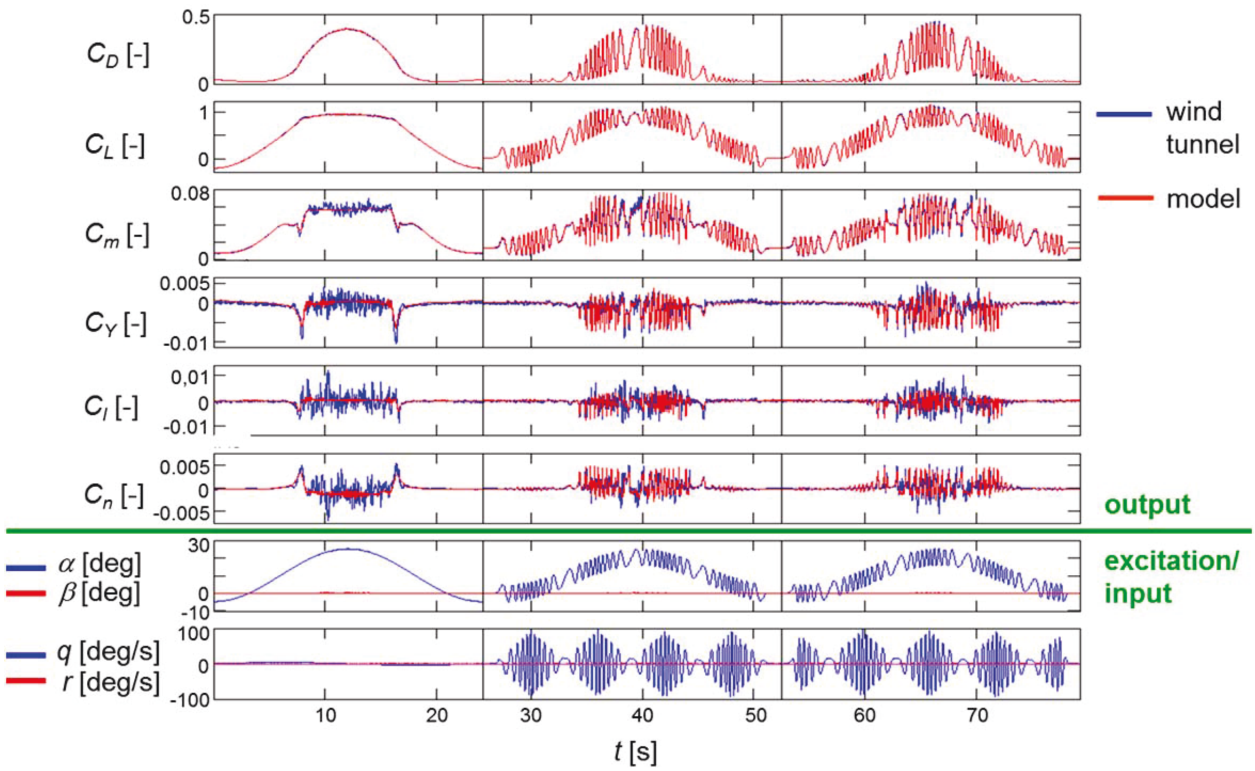

FIGURE 4. Time history fit of longitudinal quasi-static maneuver & α-frequency sweeps up/down

2.3. Results

Figure 4 shows the time history fit of the DLR-F19 longitudinal and lateral aerodynamic coefficients for a pitch axis excitation, the wind tunnel data in blue and the output of the model developed by means of system identification in red.The first time slice contains a slow quasi-static pitch maneuver, the second time slice a slow quasi-static pitch maneuver with superimposed α-frequency-sweeps starting with a slow frequency (*α*-sweep-up maneuver), and the third time slice a similar maneuver but with superimposed *α*-sweeps starting with a high frequency (*α*-sweep-down maneuver). The latter two superimposed sweep maneuvers are complementing each other in order to induce equally distributed slow and high frequencies throughout the angle of attack regime. For example, the second time slice shows a slow frequency at maximum angle of attack whereas the third time slice has a relatively high frequency at this point. The time histories clearly show the nonlinear behavior of the coefficients. Except for some noise contained in the signals at high angle of attack, the model fit is very good, simulating the essential nonlinearities.

Figure 5 shows the cross-plot fit of the pitching moment coefficient in clean configuration, in this case of the quasi-static pitch maneuver. The blue line corresponds again to the wind tunnel data, the red line displays the dynamic model output, and the green line illustrates the quasi-static portion of the model output without the hysteresis effects due to separation and re-attachment of the airflow (being intentionally small in this case). As in the time histories fit, the essential nonlinear effects are replicated, and the noise level increases with angle of attack.

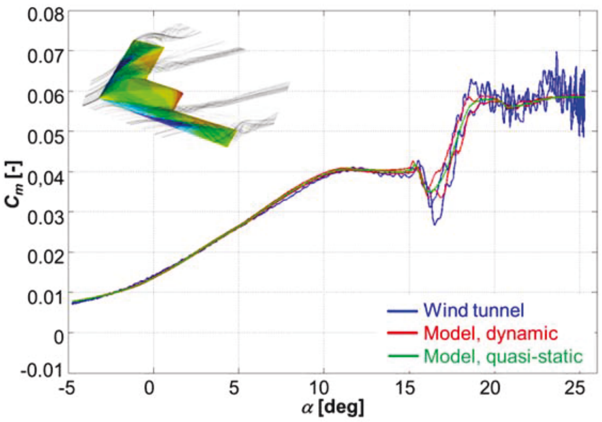

FIGURE 5. Cross-plot fit of pitching moment coefficient for the quasi-static maneuver (shown in the first time slice in Figure 4) in clean configuration

Figure 6 shows the cross-plot fit of the pitching coefficient for the quasi-static pitch maneuvers with superimposed α-sweeps, again in clean configuration. In this case the hysteresis effects due to separation and re-attachment of the airflow are significant. The quasi-static portion of the model output, shown in green, is exactly the same as in Figure 5 because all tests were evaluated in a single identification run. Now the hysteresis loops are significant but again reproduced quite well.

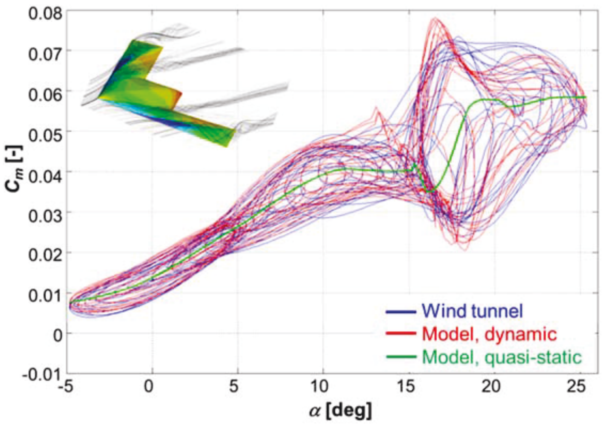

FIGURE 6. Cross-plot fit of pitching moment coefficient for the *α*-sweep-down maneuver (shown in third time slice in Figure 4) in clean configuration

The cross-plot fit of the pitching moment coefficient for quasi-static maneuvers in particular flap configurations is presented in Figure 7. The different trailing edge control surface settings do not only cause a vertical curve shift but also lead to a change in the lift curve slope.

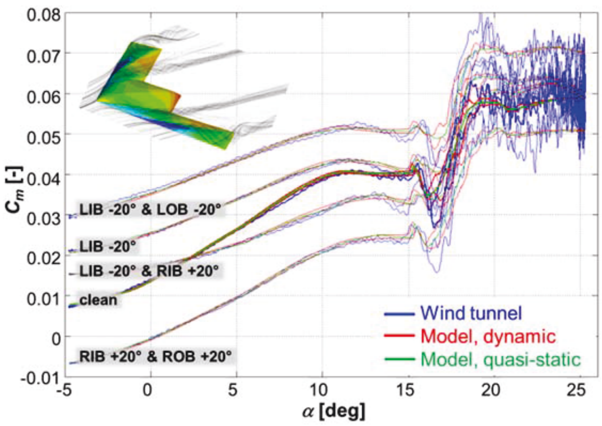

FIGURE 7. Cross-plot fit of pitching moment coefficient for quasi-static maneuvers (shown in the first time slice in Figure 4) in particular control surface configurations

The difference in the pitching moment coefficient for two different control surface deflections provides the control surface efficiency of the corresponding movable. The finally identified DLR-F19 flap efficiencies are plotted against angle of attack in Figure 8, in this case for all force and moment coefficients. The labels SP25 and SP20 denote 25% and 20% split flaps depth, both of which were used for the DLR-F19 in order to get results comparable to the DLR-F17 experiments. Figure 8 illustrates the strong dependency of the aerodynamic coefficients on the angle of attack and their strongly nonlinear behavior at moderate and high angles of attack.

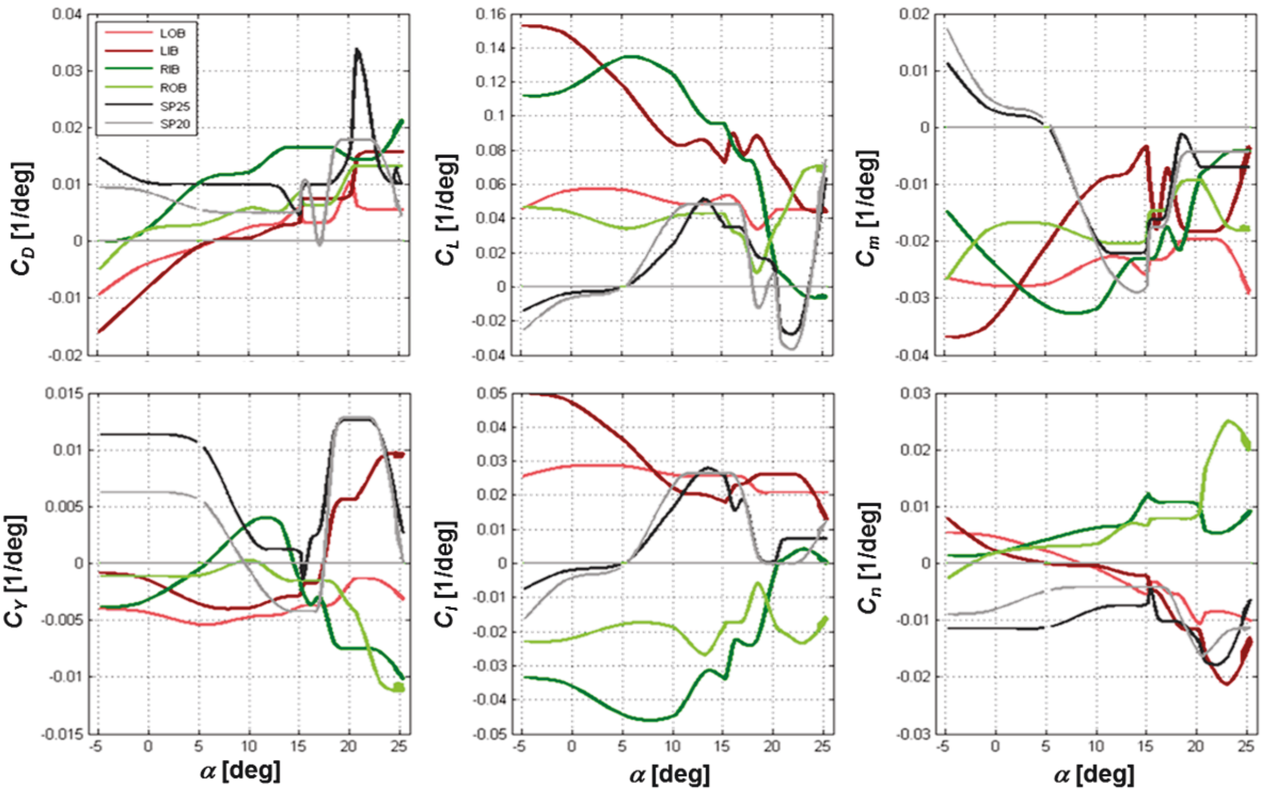

FIGURE 8. Identified DLR-F19 control surface efficiencies for the left and right inboard (LIB,RIB) and left and right outboard (LIB,LOB) control surfaces as well as split flaps with 20% (SP20) and 25% (SP25%) split flap depth

3. VSAERO AERODYNAMICS

As an example for fast and simple aerodynamic tools, the commercial VSAERO code [3] is used to get an alternative aerodynamic dataset of the present UCAV configuration. VSAERO is a 3D singularity method based on inviscid and incompressible potential flow theory, calculated on surface meshes. It computes the aerodynamic force and moment coefficients typically within a few seconds. For investigating compressible flows, several compressibility corrections are included; viscous drag can optionally be considered by an iteratively coupled boundary layer module. For damping derivative computation, quasi-steady rotations can be applied.

In the analysis presented here, VSAERO is applied on the basis of the CPACS file (cf. Section 1) of the UCAV configuration. As flow conditions, a range of Mach and Reynolds numbers as well as the angles of attack and sideslip are specified. Control surface deflections are implemented by rotation of the normal vectors of the corresponding panels around the hinge line. The option to apply viscous drag in VSAERO is not used here; instead a simple formula based on flat plate analogy is employed.

VSAERO is a well-proven tool for conventional transport aircraft. Anyway, due to the limitations of the underlying model, it is obvious that significant vortex and separation dominated effects of such a highly swept configuration – especially at higher angles of attack – cannot be modeled correctly. A detailed analysis of this aspect can be found in [1]. The question in this paper is whether a low-fidelity tool like VSAERO can already provide a reasonable first impression of the behavior and critical properties of such a configuration. Figure 9 shows a surface and wake mesh of the DLR-F19 UCAV configuration for the use with VSAERO.

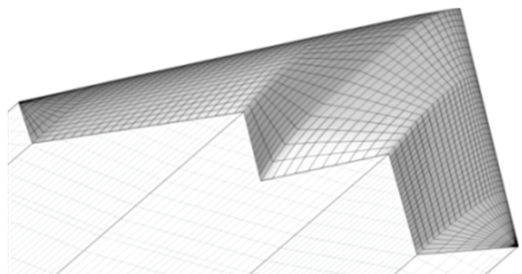

FIGURE 9. VSAERO mesh of the DLR-F19 UCAV configuration

4. FLIGHT DYNAMICS MODEL

In order to analyze and compare the flight dynamics of the overall aircraft, the aerodynamic models obtained from system identification and VSAERO are integrated into a 6-degrees-of-freedom aircraft simulation environment. This environment is called flightSim and consists of:

- a model integration process that allows for fully automatic generation of aircraft flight dynamics models from CPACS or other databases. This process is part of a standardized Dynamic Aircraft Model Integration Process (DAMIP) developed at the DLR Institute of System Dynamics and Control, see [17],
- a Modelica®-based library of aircraft models and model components that allows for automatic generation of dedicated runtime models (6-DoF, 3-DoF, forward, inverse, open loop, closed loop) for various types of model analyses (flight dynamics, performance, mission simulation, etc.), see [18] for more details.

In order to generate a flight dynamics model on the basis of the aerodynamic dataset computed by VSAERO, the standard process as applied in DLR projects like FaUSST, VAMP, and FrEACs was used, see [19]. For inclusion of the aerodynamics model obtained from system identification of wind tunnel measurements, a dedicated aerodynamics module was developed. Both simulation models are based on nonlinear Newton-Euler equations of motion for a rigid body and use the same weight and balance, systems, sensors, and engine modules. The engine modules are based on engine performance maps, which are described in detail in [20].

The simulation models feature standardized inputs (control deflections, engine throttle settings, combined control surface deflections for trimming, wind components) and outputs (states, air data sensors, inertial sensors, navigation sensors, etc.), as well as scripts for trimming and linearization. For the flying qualities analysis presented here, not all modules of the flight dynamics model are necessarily required. Components like air data or navigation sensors, for instance, are not needed for this analysis. Their integration in the model, however, allows a general use of the flight dynamics model for further assessments of the aircraft behavior.

5. FLYING QUALITIES ANALYSIS

The developed flight dynamics model is used to assess the flying qualities of the considered UCAV configuration. The flight dynamics analysis focuses on comparing the dynamic behavior of the previously determined model of the configuration derived from wind tunnel data (cf. section 2) with the dynamics of the same aircraft configuration containing the aerodynamic dataset computed with the low-fidelity aerodynamic tool VSAERO (cf. section 3).

The considered aircraft configuration for the flying qualities analysis corresponds to the DLR-F19 UCAV configuration described above. The underlying wind tunnel data, however, result from the predecessor wind tunnel model, the NASA built SACCON, which has an identical outer shape but smaller flaps on the trailing edge compared to the DLR-F19 configuration. The control surfaces of the SACCON model only cover 20% of the wing chord compared to 25% for the DLR-F19 model. Thus, the CPACS model of the DLR-F19 configuration was modified for the VSAERO computations in order to have the same chord of the control surfaces as the SACCON model.

5.1. Framework of Flying Qualities Analysis

The selection of appropriate criteria for the assessment of the flight dynamic behavior of an UCAV configuration is generally problematic because the established handling and flying qualities criteria apply to manned air vehicles. The main purpose of these criteria is to assess whether an aircraft can be handled by a human pilot. This aspect is obviously irrelevant for an unmanned vehicle like the considered configuration. Nevertheless, commonly used flying qualities criteria of conventional, manned aircraft are applied here to get a general impression of the flight dynamic behavior of the considered aircraft. Even though the exact limits for specific flying qualities level are irrelevant for the UCAV configuration the application of the criteria gives a good qualitative impression of the dynamics of the aircraft. The purpose of the analysis it to compare the behavior obtained with the two different aerodynamic datasets instead of a quantitative assessment of the flying qualities with a determination of the exact flying qualities levels.

The flying qualities analysis is performed with the analysis tool HAREM (HAndling qualities Reasearch using Matlab) [21], [22]. This tool was developed at the Institute of Flight Systems of DLR and allows the assessment of a wide range of handling and flying qualities criteria in an automatic manner. It applies the criteria to linear flight dynamics aircraft models and automatically delivers the corresponding flying qualities level as well as figures showing the criterion graphs. For the presented results HAREM has been integrated into a workflow, in which the tool flightSim (cf. section 4) generates a flight dynamics model of the UCAV configuration and passes this to HAREM as a CPACS file. A detailed description of the application of HAREM in combination with CPACS is given in [23].

The flight dynamics analysis of the UCAV configuration is performed for the full-size model of the aircraft with the characteristics shown in Table 1. Actuator dynamics as well as automatic flight control are not considered for the flying qualities analysis.

Aircraft Parameter	Value
Wing area	77 m²
Span	15.4 m
Aircraft mass	13.9 t
Moment of inertia I_{xx}	91122 kg m²
Moment of inertia I_{yy}	31560 kg m²
Moment of inertia I_{zz}	122682 kg m²

TABLE 1. Characteristics of UCAV configuration

For the application of the flying qualities criteria of HAREM the flight phase and aircraft category of the considered configuration have to be defined according to the specifications of MIL-STD-1797 [24]. The flight phase is defined by the conditions of the wind tunnel experiments. As the experiments have been performed at a Mach number of 0.15, the resulting aerodynamic dataset is valid for the low-speed range only. These airspeeds occur only during takeoff, approach and landing. The corresponding flight phase category C of MIL-STD-1797 is thus considered for the analysis. The flight condition underlying the present flying qualities analysis is a trimmed horizontal flight at 500 m altitude with a calibrated airspeed of 100 m/s, which corresponds to a Mach number of 0.3. At this Mach number compressibility effects are still negligible such that the aerodynamic dataset determined by low speed wind tunnel experiments is still valid. Both aircraft classes II and IV are considered in the analysis. Class II is considered because the currently specified mission of the UCAV configuration contains comparably moderate maneuvers for a fighter aircraft. This correlates to the definition of aircraft class II for medium weight aircraft with low to medium maneuverability. For future applications, however, the UCAV configuration may be used as a highly agile fighter aircraft. The flying qualities are thus also assessed for aircraft class IV covering high maneuverability aircraft.

The flying qualities level used here correspond to the definitions of [24]. Level 1 denotes "Satisfactory" flying qualities, level 2 means the flying qualities are "Acceptable", and level 3 describes "Controllable" flying qualities. As already mentioned, however, the exact flying qualities level is not relevant here because an unmanned configuration is considered. The analysis shall only give a qualitative impression of the dynamic behavior of the UCAV and show the comparison of the two aircraft models using aerodynamic datasets derived with different methods.

5.2. Longitudinal Dynamics

The UCAV configuration was designed to be stable in the longitudinal axis. The two aerodynamic datasets yield, however, different static margins. In case of the VSAERO dataset the static margin is 9.8% of the mean aerodynamic chord. The model derived from the wind tunnel data, in contrast, has a static margin of 3.2%. The center of gravity is identical for both models. The VSAERO computations deliver, however, an aerodynamic neutral point that is located significantly further aft compared to the neutral point position derived from the wind tunnel measurements. The absolute deviation between the neutral point positions is relatively small; as the neutral point positions are located very closely to the center of gravity of the aircraft, which is typically the case for a tailless aircraft, the resulting effect for the stability margin is significant though. The same trend has been found when comparing the VSAERO results with high-fidelity CFD results [2].

The larger static margin resulting from the VSAERO computations also leads to a larger absolute value of angle-of-attack dependent pitching moment derivative $C_{m\alpha}$ and consequently to a higher natural frequency of the short period dynamics of the aircraft. The aircraft model based on the VSAERO results has a $C_{m\alpha}$ of -0.30, whereas the $C_{m\alpha}$ of the aircraft model derived from the wind tunnel data is -0.08. The resulting higher natural frequency of the VSAERO based model effects a higher agility in the longitudinal axis compared to the aircraft model with aerodynamic data from the wind tunnel experiment. This effect is visible in the criterion graph of the Control Anticipation Parameter (CAP) illustrated in Figure 10.

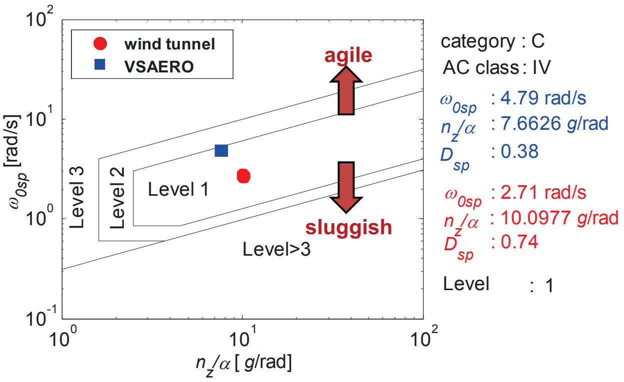

FIGURE 10. Comparison of the flying qualities levels of the CAP criterion achieved for the two aircraft models with different aerodynamics datasets

The CAP criterion assesses the initial pitch acceleration in relation to a steady change of the vertical load factor. If this ratio is very large, the aircraft is very agile in the longitudinal axis. It can be noticed in Figure 10 that, even though the VSAERO based model is located at higher natural frequencies in the CAP criterion graph, it is still placed in the Level 1 region. The damping ratio of the short period mode is lower for the model based on VSAERO computations than for the aircraft model determined on the basis of the wind tunnel measurements. This is another indicator that the VSAERO based aircraft model exhibits more agile dynamics in the longitudinal axis.

The higher agility of the VSAERO based model compared to the wind tunnel experiment based model is also visible in the criterion graph of the *C** criterion (Figure 11). The *C** criterion [25] specifies requirements for the maximum allowable overshoot in the time response of the parameter *C** after a step input in the pitch axis. The *C** parameter is defined as a combination of the vertical load factor at the pilot seat and the pitch rate of the aircraft:

$$C^* = \left(n_{z,pilotseat} + \frac{1}{g}240\text{kt} \cdot q\right). \quad (1)$$

The factor of 240 kt represents the so-called crossover speed, at which the load factor and pitch rate component of C* are equally weighted. The parameter $n_{z,pilotseat}$ corresponds to the vertical load factor at the position of the pilot seat. As there is no pilot in the UCAV configuration the vertical load factor at the center of gravity is considered here instead. The *C** criterion is usually applied for civil, manned aviation. Nevertheless, it gives a very good impression of the agility of an aircraft in the longitudinal axis.

Figure 11 shows that the VSAERO based aircraft model has a strong overshoot in the *C** response and is too agile. This is not very critical as the badly damped, too agile *C** response can easily be improved by an appropriate flight control system. The important observation derived from Figure 11 is the fact that the *C** response of the two models with different aerodynamics datasets is significantly different. This is important to note during the aircraft design process. If only the low-fidelity aerodynamic method were applied this would give the impression of a much more agile aircraft than it might be the case in reality.

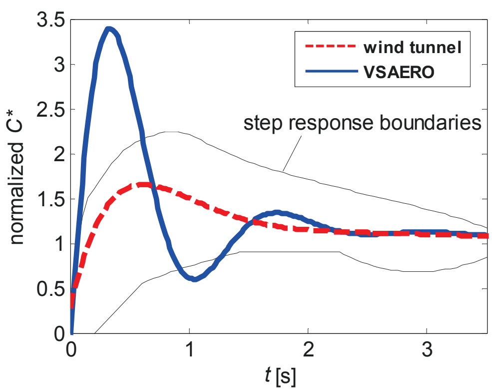

FIGURE 11. Comparison of the flying qualities levels of the *C** criterion for the two aircraft models with different aerodynamics datasets

5.3. Lateral Dynamics

The comparison of the eigenvalues of the lateral-directional motion in Figure 12 already shows that the different aerodynamic methods also lead to different lateral-directional dynamics.

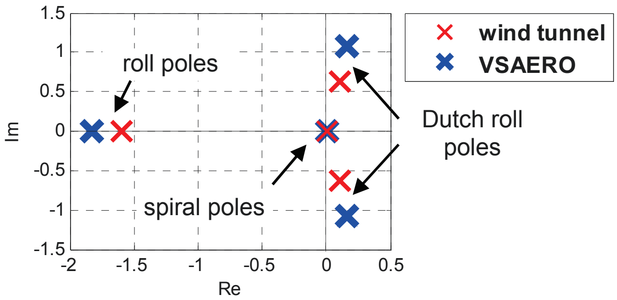

FIGURE 12. Eigenvalues of the lateral-directional motion for the two aircraft models with different aerodynamics datasets

The spiral poles are located comparably close to each other, but especially for the roll and Dutch roll poles the difference of the two aerodynamic methods is clearly visible. Nevertheless, both aircraft models achieve the same flying qualities level concerning the different criteria for the lateral-directional eigenmodes. Table 2 shows that the roll time constant fulfills the requirements for level 1 flying qualities in both cases. However, the aircraft model containing the VSAERO dataset exhibits better flying qualities. The slightly smaller roll time constant of the UCAV model with the aerodynamic dataset from VSAERO results from the fact that the VSAERO dataset exhibits a larger absolute value of the roll damping derivative C_{lp}, which is inversely proportional to the roll time constant. The higher roll damping can be explained by the fact that VSAERO overestimates the lift curve slope, which has also been shown in [2]. As the VSAERO computations are based on inviscid and incompressible potential flow theory, they cannot properly model the complex flow field of a configuration with highly swept leading and trailing edges.

	Roll time constant
Maximum value for level 1	1 s
VSAERO dataset	0.57 s
Wind tunnel dataset	0.67 s

TABLE 2. Roll time constants for the two aircraft models with different aerodynamics datasets

The spiral mode is unstable for both aerodynamic datasets, but the instability is only small and the requirements for the time to double of 12 s for level 1 flying qualities can easily be fulfilled, as shown in table 3. As in the case of the roll time constant, the VSAERO approach delivers slightly better flying qualities. The reason for the difference in the times-to-double of the two aircraft models still needs to be investigated in detail. The consequences are, however, small because the margin to the given threshold value of 12 s is large in both cases.

	Time to double
Minimum value for level 1	12 s
VSAERO dataset	131 s
Wind tunnel dataset	54 s

TABLE 3. Time to double amplitude of the spiral motion for the two aircraft models with different aerodynamics datasets

The criterion graph for the Dutch roll mode is shown in Figure 13. For both aerodynamic datasets the UCAV configuration exhibits Dutch roll dynamics corresponding to a flying qualities level worse than 3 because the configuration has a negative damping and is dynamically unstable. Moreover, the natural frequency of the Dutch roll is very low for both aerodynamic datasets. In case of the VSAERO based model the natural frequency is still slightly higher because the yaw moment derivative with respect to the sideslip angle is slightly higher, as also demonstrated in [2]. The unfavorable Dutch roll dynamics were expected because the considered UCAV configuration does not possess a stabilizing vertical tail nor any kind of fins. Concerning the unstable Dutch roll motion the relevant question is whether a flight control system is able to stabilize the dynamics in the lateral-directional axes. This depends on the available control authority of the control surfaces and can be assessed with the closed-loop model of the aircraft, which is, however, out of the scope of the paper.

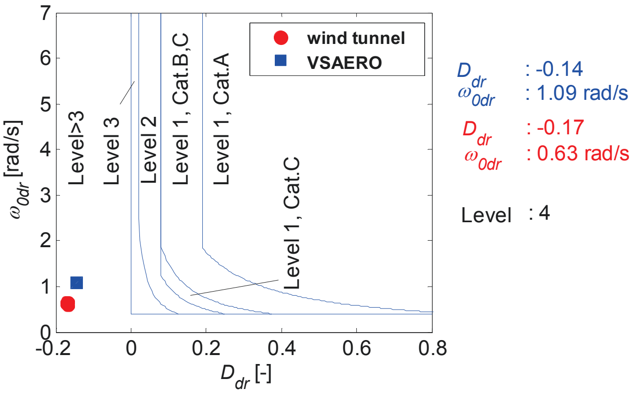

FIGURE 13. Comparison of the flying qualities levels of the Dutch roll characteristics for the two aircraft models with different aerodynamics datasets

The requirements for the roll performance as specified by [24] are illustrated in Figure 14. It shows the time response of the two aircraft models with different aerodynamic datasets for maximum roll control input. The considered UCAV configuration has two trailing edge control surfaces on each wing. In the presented case only the outer control surfaces are used for roll control.

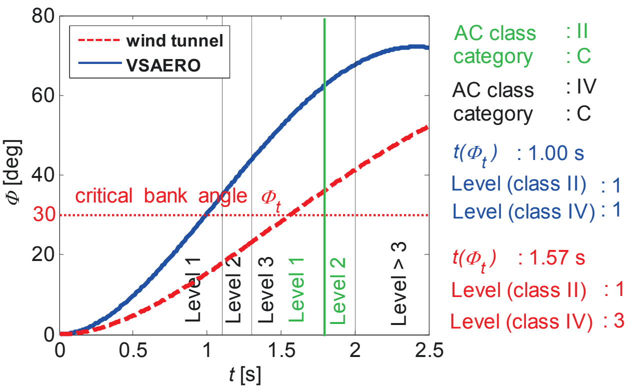

FIGURE 14. Comparison of the flying qualities levels of the roll performance for the two aircraft models with different aerodynamics datasets

Depending on the flight phase category and aircraft class, [24] defines time periods in which specific bank angle values have to be reached. In flight phase category C a class II aircraft (land-based) has to be able to reach a bank angle of 30° within 1.8 s to be classified as level 1. The corresponding limit is marked with a green line in Figure 14. If the aircraft is considered as a high maneuverability aircraft of class IV it has to reach a 30° bank angle in 1.1 s for level 1 flying qualities. The corresponding limits for class IV aircraft are shown in black in Figure 14.

The comparison of bank angle responses of the VSAERO and wind tunnel experiment based aircraft model shows that the VSAERO based model is once again much more agile and has a significantly better roll performance. If the UCAV is evaluated as a class II aircraft the wind tunnel based model still fulfills level 1 requirements. If the UCAV is to be used as an agile fighter aircraft of class IV, however, the roll performance is too low and only corresponds to level 3. The VSAERO based model, in contrast, reaches level 1 flying qualities as a class IV aircraft as well. The reason for the worse roll performance of the aircraft model derived from the wind tunnel data is the fact that a lower roll effectiveness was detected in the wind tunnel experiment than it was predicted by the VSAERO method. The VSAERO method delivered a roll control dependent roll moment derivative $C_{l,ail}$ of -0.14 whereas the wind tunnel experiment provided a $C_{l,ail}$ of -0.06. The overestimation of the efficiency of the control surfaces by VSAERO was expected because the potential flow theory based computation method assumes attached flow and thus predicts full efficiency of the control surfaces. In reality the control surface efficiency is significantly reduced due to flow separation and vortex effects. Moreover, the way how the aerodynamic performance map is stored in CPACS is based on linear superposition of separate control surfaces. This method neglects the cross-influences between different control surfaces. This is a valid approach for conventional transport aircraft; however, as shown in [27], these effects are not negligible for the considered UCAV configuration. A detailed comparison of the VSAero results with high-fidelity CDF computations and wind tunnel experiments can be found in [2].

The fact that the roll performance determined on the basis of the wind tunnel experiment is so much smaller could be a critical aspect for the UCAV design if a high roll maneuverability is desired for the later application of the UCAV. It has to be kept in mind, however, that only the outer trailing edge control surfaces on the wing are used for the roll control here. Even though the inner trailing edge control surfaces are less effective due to their small lever arm, an increased roll performance could be achieved by deflecting them simultaneously with the outer control surfaces. It should thus be considered to use all trailing edge control surfaces for dynamic roll maneuvers, provided sufficient longitudinal control power remains.

As the considered UCAV configuration without vertical fins is expected to be unstable in the yaw axis, the dynamics in this axis are particularly considered in the flight dynamics assessment of this aircraft. [26] suggests requirements for the dynamics in the directional axis which shall assure that an unstable aircraft can be stabilized by an automatic flight control system. [26] defines that the time to double the amplitude of the sideslip angle should be larger than 350 ms. In this approach it is assumed that the dimensional side force derivatives with respect to sideslip angle and rudder deflection as well as dimensional yaw moment derivative with respect to yaw rate in the aerodynamic coordinate system are negligible:

(2) $$Y_\beta \approx Y_{rud} \approx N_{r_a} \approx 0 \, .$$

This allows the following approximation for the time to double of the sideslip angle

(3) $$T_2 = \frac{\text{acosh}(2)}{\sqrt{-N_{\beta_a}}} \, ,$$

with N_{β_a} representing the dimensional yaw moment derivative with respect to sideslip angle in aerodynamic axes. All dimensional derivatives are defined according [28], i.e. correspond to the respective force or moment derivative divided by the mass or moment of inertia. Directional stability requires a positive value of the parameter N_{β_a}, given in the aerodynamic coordinate system. The dimensional derivative N_β in body-fixed coordinates is negative for both aerodynamic datasets. However, the transformation into the aerodynamic coordinate system leads to a positive (i.e. stable) dimensional yaw moment derivative at the considered trim point because of the influence of the stable (i.e. negative) dimensional roll moment derivative with respect to sideslip angle L_β:

(4) $$N_{\beta_a} = N_{\beta_b} \cos(\alpha) - L_{\beta_b} \sin(\alpha).$$

At the considered trim point with a Mach number of 0.3 the angles of attack of 6.3° in case of the VSAERO based model and 7.4° in case of the wind tunnel data based model are large enough to ensure a stable directional motion thanks to the influence of L_β. At larger Mach numbers the influence of L_β becomes smaller due to the smaller angle of attack. Larger Mach numbers, however, cannot be reliably assessed with the available dataset because the wind tunnel data is only valid for the low speed range. An extrapolation of the available dataset to a Mach number of 0.5 with trimmed angles of attack of 3.3° (wind tunnel dataset) and 2.7° (VSAERO dateset) suggests that the UCAV would be slightly unstable at this Mach number with times to double amplitude of the sideslip angle of 3.4 s for the VSAERO based model and 3.0 s for the wind tunnel based model. Both values are well above value of the minimum time-to-double of 350 ms required in [26]. This suggests that the instability of the UCAV might still be acceptable at the Mach number of 0.5. These results as well as the instability for the high speed range need, however, to be verified with appropriate aerodynamic data, which is valid for the corresponding Mach numbers.
What extent of instability can actually be compensated by an active flight control system depends on several parameters like the available control power, moments of inertia and time delays and the actuators and control system. The sensitivities with respect to these parameters will be analyzed in future studies.

6. CONCLUSIONS

The current paper presents an innovative way to derive a flight dynamics model from wind tunnel data by means of a system identification approach. This is based on the combination of the dynamic capabilities of the Model Positioning Mechanism (MPM) at DNW-NWB and the system identification expertise at the DLR Institute of

Flight Systems. New quasi-steady maneuvers with superimposed harmonic excitation or frequency sweeps are applied via the MPM and then evaluated with a nonlinear system identification tool. The main benefits compared to classical linear evaluation methods are the ability to model highly nonlinear aerodynamic behavior and a substantially reduced number of wind tunnel measurements in order to generate results for a complete 6-DoF envelope within the wind tunnel hardware limits. The wind tunnel time saving depends on the test program, but can exceed 75%.

The comparison of the flight dynamics model derived from the wind tunnel experiments with a flight dynamics model with aerodynamic data determined with VSAERO shows that even the application of linear flying qualities criteria yields some significant differences between the two aerodynamic datasets. In the longitudinal axis the VSAERO based model is much more agile than the wind tunnel data based model. This behavior results from the fact that positions of the aerodynamic neutral point differ for the two aerodynamic datasets. Concerning the lateral-directional dynamics of the UCAV it could be noticed that the aerodynamic dataset determined with VSAERO leads to better flying qualities for all criteria applied in the present analysis. Even if the differences for the lateral-directional eigenmodes are not very large, a more significant deviation between the dynamic behaviors of the two models could be identified concerning the achievable roll performance. The VSAERO based model provides sufficient roll performance to achieve level 1 flying qualities as a highly maneuverable aircraft of class IV, whereas the wind tunnel experiment based aircraft model only reaches level 3 flying. The observed effect that VSAero overestimates the efficiency of the control surfaces was expected due to the underlying assumptions of inviscid and incompressible potential flow theory and the simplified linear superposition of separate control surface deflections specified in the employed CPACS interface. Nevertheless, the overestimation of the efficiencies always has to be kept in mind for the evaluation of the VSAREO based data.

In order to improve the roll performance and achieve level 1 flying qualities for class IV aircraft as well, it should be considered to apply both trailing edge control surfaces on each wing for roll control – as far as permitted by necessary longitudinal control – to increase the roll maneuverability of the UCAV.

Altogether the flying qualities of the DLR-F19 configuration can be rated as satisfactory considering the fact that the configuration was analyzed without any kind of automatic flight control. A detailed analysis of the closed-loop system with active flight control still has to be performed for a final assessment of the configuration, however. This analysis is part of the ongoing studies at DLR. A description of the control laws can be found in [19].

The observed differences between the dynamics resulting from the two aerodynamic datasets support the assumption that low-fidelity aerodynamic computations with VSAERO are not sufficient to adequately model the aerodynamic behavior of such a flying wing configuration with highly swept leading and trailing edges and low aspect ratio. On the other hand, the results show that some critical issues of the configuration can already be identified with such simple methods, even if the absolute values show significant deviations from high-fidelity data. However, it is essential to be aware of the fact that the results obtained with VSAERO do not cover all relevant physical effects and might thus yield better flying qualities than the aircraft exhibits in reality.

This underlines the continued usefulness of costly high-fidelity CFD computations or wind tunnel experiments to extract accurate aerodynamics and flight dynamics. A way to improve the efficiency of the process is the approach presented in this paper with innovative wind tunnel maneuvers followed by nonlinear system identification.

ACKNOWLEDGMENTS

The authors would like to thank all colleagues of the DLR project FaUSST who contributed to the work presented here. They especially appreciate the contributions of the colleagues of the DNW-NWB for performing the wind tunnel experiments and the colleagues from the DLR Institute of Propulsion Technology for providing the engine performance map for the UCAV model.

REFERENCES

[1] Cummings, R. M., Schütte, A.: *An Integrated Computational/Experimental Approach to UCAV Stability & Control Estimation: Overview of NATO RTO AVT-161*, 28th AIAA Applied Aerodynamics Conference, AIAA-2010-4392, Chicago, IL, USA, June 2010.

[2] Liersch, C. M., Huber, K.: *Conceptual Design and Aerodynamic Analyses of a Generic UCAV Configuration,* 32nd AIAA Applied Aerodynamics Conference, AIAA-2014-2001, Atlanta, GA, USA, June 2014.

[3] Nathman, J. K.: *VSAERO – A Computer Program for Calculating The Nonlinear Aerodynamic Characteristics Of Arbitrary Configurations*, Users' Manual Version 7.2, Redmond, WA, USA, September 2007.

[4] Nagel, B., Böhnke, D. Gollnick, V. , Schmollgruber, P., Rizzi, A., La Rocca, G., Alonso, J. J.: *Communication in Aircraft Design: Can we establish a Common Language?*, 28th International Congress of the Aeronautical Sciences, Brisbane, Australia, 2012.

[5] Bergmann, A.: *The New Aeroacoustic Low Speed Facility DNW-NWB*, 18th AIAA/CEAS Aeroacoustics Conference, AIAA-2012-2173, Colorado Springs, Colorado, USA, 4-6 June 2012.

[6] Pott-Pollenske, M., von Heesen, W. , Bergmann, A.: *Acoustical Preexamination Work and Characterization of the Low Noise Wind Tunnel DNW-NWB*, 18th AIAA/CEAS Aeroacoustics Conference, AIAA-2012-2175, Colorado Springs, Colorado, USA, 4-6 June 2012.

[7] Loeser, T., Schröder, E.: *The Anechoic Plenum of the DNW-NWB Aeroacoustic Wind Tunnel,* 18th AIAA/CEAS Aeroacoustics Conference, AIAA-2012-2179, Colorado Springs, Colorado, USA, 4-6 June 2012.

[8] Bergmann, A.: *Modern Wind Tunnel Techniques for Unsteady Testing – Development of Dynamic Test Rigs*, in: *Hermann Schlichting – 100 Years*, Springer, Braunschweig, Germany, 2009, pp. 59-77.

[9] Cummings, R. M., Schütte, A.: *The NATO STO AVT-201 Task Group "Extended Assessment of Stability and Control Prediction Methods for NATO Air Vehicles"*, 32nd AIAA Applied Aerodynamics Conference, AIAA-2014-2394, Atlanta, GA, USA, June 2014.

[10] Vicroy, D., Huber, K., Rohlf, D., Loeser, T.: *Low-speed Dynamic Wind Tunnel Test Analysis of a Generic 53° Swept UCAV Configuration*, 32nd AIAA Applied Aerodynamics Conference, AIAA-2014-2003, Atlanta, GA, USA, June 2014.

[11] Loeser, T.: *Experimental Research of Dynamic Derivatives of Unsteady Moved Aircraft*, in: *Experimental Determination of Dynamic Stability Parameters*, VKI LS 2008-02, Rhode-St-Genèse, Belgium, 2008.

[12] Rohlf, D., Schmidt, S., Irving, J.: *Stability and Control Analysis for an Unmanned Aircraft Configuration Using System-Identification Techniques*, J. Aircraft, Vol. 49, No. 6, Nov-Dec 2012.

[13] Loeser, T., Rohlf, D.: *Experimental Determination of Dynamic Derivatives in a Wind Tunnel using Parameter Identification*, in: *New Results in Numerical and Experimental Fluid Mechanics X*, 19th STAB/DGLR Symposium Munich, Germany, 2014.

[14] Seher-Weiß, S.: *User's Guide: FITLAB Parameter Estimation Using MATLAB - Version 2.0,* DLR-Internal Report, DLR-Internal Report, 111-2007/27.

[15] Fischenberg, D.: *Identification of an Unsteady Aerodynamic Stall Model from Flight Test Data*, AIAA Paper 95-3438, August 1995.

[16] Jategaonkar, R. V.: *Flight Vehicle System Identification: A Time Domain Methodology*, Vol. 216, AIAA Progress in Astronautics and Aeronautics Series, AIAA, Reston, VA, USA, 2006.

[17] Kier, T., Looye, G., Scharpenberg, M., Reijerkerk, M.: *Process, methods and tools for flexible aircraft flight dynamics model integration*, International Forum on Aeroelasticity and Structural Dynamics, Stockholm, Sweden, 2007.

[18] Looye, G.: *The New DLR Flight Dynamics Library,* in: Proceedings, 6th Modelica Conference, 2008-03-03 - 2008-03-04, Bielefeld, Germany, 2008.

[19] Kuchar, R., Steinhauser, R., Looye, G.: *Design of Flight Control Laws for Agile and Highly Swept Aircraft Configurations,* accepted for the DGLR Jahrestagung 2015, Rostock, Germany.

[20] Nauroz, M., Becker, R., Robinson, J.: *Individual Effects of Components on Cycle/Propulsive Efficiency for Variable Cycle Engines* Deutscher Luft- und Raumfahrtkongress 2012, Berlin, Germany, 10-12 September 2012.

[21] Duus, G., Duda, H.: *HQML: Ein Programmpaket zur Flugeigenschaftsanalyse unter MATLAB,* DLR-Internal Report, 111-97/22, 1997.

[22] Duus, G.: *Überarbeitung des HAREM Programm-pakets*, DLR-Internal Report, 111-2001/10, 2001.

[23] Ehlers, J.: *Flying Qualities Analysis of CPACS Based Aircraft Models*, DLR-Internal Report, 111-2013*/21, June 2013.*

[24] *N.N.: Mil-STD Military Standard, Flying Qualities of Piloted Aircraf*t, MIL-STD-1797A, 1990.

[25] Tobie, H.N.: “A new longitudinal handling qualities criterion”, Boeing Company, 1967.

[26] Osterhuber, R.: *FCS Requirements for Future LO Combat Aircraft*, STO/AVT-215 Workshop on “Innovative Control Effectors for Military Vehicles”, Stockholm, Sweden, 20-22 May 2013.

[27] Huber, K., Vicroy, D., Schütte, A., Hübner, A.-R.: *UCAV model design and static experimental investigations to estimate control device effectiveness and S&C capabilities*, 32nd AIAA Applied Aerodynamics Conference, AIAA-2014-2002, Atlanta, GA, USA, June 2014.

[28] Stevens, B., Lewis, F.: *Aircraft Control and Simulation*, John Wiley & Sons, New York, USA, 1992.